[SSC21-VIII-04]

A wave physics approach to electronically steerable antennas

Jean-Baptiste Gros, Vladislav Popov, Mikhail Odit, Geoffroy Lerosey
Greenerwave
6 rue Jean Calvin, 75005 Paris, France; +33 1 40 79 43 28
geoffroy.lerosey@greenerwave.com

ABSTRACT

Electronically steerable antennas, that are compact, thin, light and contain no mechanical parts, are being more and more used for satcom applications on the ground, notably owing to the fast development of mega constellations; yet their use is still very limited on board. Indeed, all designs up to date rely on the same old concept, phased arrays, namely, a large number of sources that are phased matched to point in various directions. These can be passive, in the sense that a common feed is used to radiate through many radiators, or active in which case each tiny emitter contains its own source of waves. While the former are relatively simpler and less energy greedy, they are very dissipative and hence of poor efficiency. The latter, on the contrary, often offer good performances, yet they are extremely costly and require huge amounts of electrical power to operate, the vast majority of which is dissipated into heat. In a nutshell, both active and passive phased arrays have tremendous problems when it comes to space applications.

Here we introduce the concept of the reconfigurable leaky cavity antenna, that stems on a radically different approach to beamforming. It uses a thin leaky cavity that, when excited by one or several feeds, can establish any desired wavefield corresponding to any desired radiation pattern. To achieve this, the cavity is reconfigured in real time by an electronically reconfigurable intelligent surface (metasurface). The latter controls the reflections of the waves inside the cavity, acting as a software-controlled set of boundary conditions. Being based on discrete components, the antenna maintains the cost-efficiency, robustness and power sobriety of the simplest passive phased arrays, with a power needed for beamforming as low as a few tens of watts at Ku or Ka. In the meantime, since the control is solely based on electronics, it achieves the performances of active phased arrays at the same time, for instance in terms of gain or switching speeds. With its high performances and low complexity, our concept paves the way to the deployment of electronically steerable antennas on board.

Further, since the beamforming does not result from the synchronization of many elementary sources, but rather on the shaping of a wavefield inside a cavity, our concept is standard or protocol agnostic. Moreover, it is able to support multiple frequency bands, and to emit multiple beams, at different frequencies and with different polarization.

INTRODUCTION

Beamforming is a technique that dates back to the beginning of the 20th century, with the initial works of Braun[1] and Marconi[2] who showed independently that using multiple antennas allowed to reinforce signal emission in one direction while minimizing it in other ones. The technique has mostly been reserved to military applications for decades, due in part to the high cost of the associated hardware and in part to the low frequencies then used for wireless transmissions. Yet it is now starting to be widely adopted in wireless systems, since ever increasing amounts of wireless data impose a better usage of bandwidth and hence spatial multiplexing, and because its cost has decreased over time, allowing real life implementation. For millimeter waves, which are at the core of 5G and satellite communications systems, it is even mandatory as waves at these frequencies need to propagate in the form of beams, akin to optics, to ensure a sufficient signal to noise ratio for efficient data transmission.[3,4]

In a typical beamforming antenna, the signal is carried by waves that are generated by a multiplicity of sources, each of which being tuned in phase and amplitude such that they interfere constructively in a given direction.[5] As a result, the energy emitted in this direction is much larger than that in other ones, resulting in a radiation pattern that presents a beam-like shape in the favored direction. In an electronically steerable antenna, these multiple independent sources are controlled in time, to modify

the direction of emission at will, or even to beam in multiple directions. These antennas, also called phased arrays,[6–8] can be classified into two types: passive and active phased arrays. Passive phased arrays, on the one hand, receive their radiofrequency waves from a common feed, which is distributed to each source, the latter being able to tune in phase and/or amplitude the portion of the wave field that it emits. In typical passive phased arrays antennas, the routing of electromagnetic energy is realized using microstrip circuits which induce at high frequency a large dissipation. The phase tuning relies on electronic components named phase shifters, that can be quite complex and costly if precision is required. Other designs such as leaky wave phased arrays involve parallel plate waveguiding, which tend to mitigate the dissipation due to the routing of the electromagnetic energy. In this case each radiator can be impedance tuned using liquid crystals,[9] at the cost of large dissipation, or can rely again on phase shifters, with the same complexity issues as above. Overall, passive phased arrays offer poor efficiencies and performances, unless complexity and cost is drastically increased.

Active phased arrays, on the other hand, generate the radiofrequency waves to be emitted locally, at each emitter, using so called monolithic microwave integrated circuits (MMIC).[10,11] Again, two approaches coexist to do so. In the first one, the low frequency waves carrying the information, typically in the GHz range, are routed using microstrips to each MMIC that is used to up(down)-convert the waves to the mmWave range, phase/amplitude tune it, and amplify it so that a connected radiator can emit/receive it. In this approach, the streams of data are sent to each MMIC in real time to shape the radiation pattern of the antenna, resulting in a frequency dependent beamforming that severely reduces the bandwidth. Another solution is to generate and measure the low frequency signals on-substrate, using large computing chips such as ASICs and FPGAs, and to distribute it to neighboring MMICs for up(down)-conversion, control and amplification. This solution, if it is even more complex and costly than the previous one, offers the advantage of larger bandwidth due to the possibility of frequency dependent phase and amplitude control. Active phased arrays, because of their high complexity, often offer relatively good performances, in terms of radiation pattern, speed, and flexibility. On the other hand, they are costly since custom MMICs must be developed and used by hundreds to thousands to realize an antenna. Furthermore, since the electrical efficiency of these MMIC is extremely poor - typically in the few percent- they consume enormous amounts of energy and often require custom cooling systems.

Whether they are active or passive, phased arrays also share the same drawbacks that are due to their intrinsic design. Indeed, these antennas emit waves using arrays of controlled yet identical elementary radiators. Hence, their radiation pattern and performances are inherently limited by that of the replicated elementary antenna that is printed on a substrate. Such an antenna has severe limits in terms of angles of emission that are naturally inherited by the phased array. Notably, the gain of these systems is much lower at wide scan angles, because the radiators simply cannot emit at these angles. Furthermore, and for the same reasons, phased arrays cannot maintain good polarization purities at wide angles, since their unitary element is not capable of doing so, hence resulting in even lower performances.

Solving at once all the issues related to phased arrays, active or passive, requires a radically new thinking of beamforming, and this is what brings Greenerwave with its electronically reconfigurable leaky cavity antenna. In the first part of the paper, we introduce the concept of our antenna, and explain how it -by design- brings a lot of advantages, in terms of simplicity, conformability, power consumption, robustness, etc... Then, we show results demonstrating that this antenna has equal or superior characteristics compared to the best phased arrays, whether it is in terms of efficiency, scan loss, bandwidth, or angular resolution. Finally, in the last part of the paper, we outline some very peculiar properties of the antenna, that are unique to it, and which allow for an unprecedented flexibility, namely controllable polarization, multi streaming capabilities, absence of beam squint and so on.

LEAKY CAVITY ANTENNA

The concept of the leaky cavity antenna is described in Figure 1. A tunable metasurface or reflectarray, consisting of an array of patch reflectors controlled by PIN diodes,[12] is placed inside a metallic cavity, preferably on the lower interface. Feeds are placed inside the cavity, such as monopoles or leaky waveguides, to inject/take out electromagnetic energy. One or more of the cavity interfaces are made leaky, using a semi-transparent mask, so that some energy leaves the cavity. In the case of Figure 1, the upper interface leaks the wavefield generated inside the cavity.

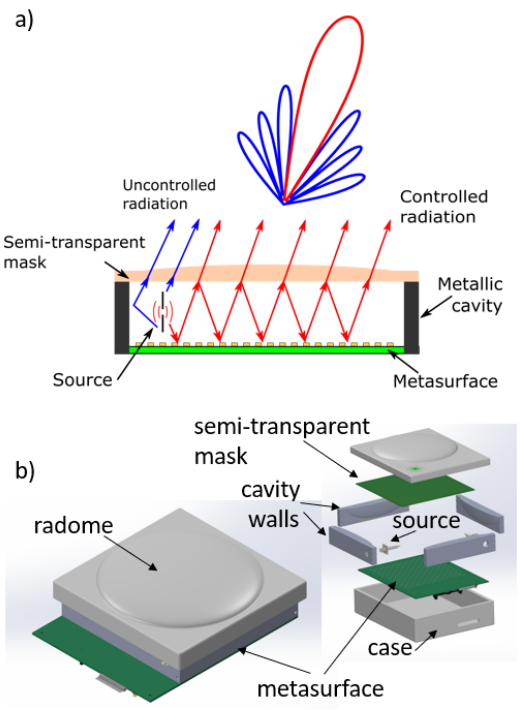

Figure 1: Schematic (a) and 3D (b) view of an electronically reconfigurable leaky wave antenna.

Waves which are initially emitted inside the cavity by a feed, establish a given wavefield following the geometry and boundary conditions of the cavity. The tunable metasurface is then modified, in order to change the artificial boundary conditions of the cavity and establish a new wavefield inside it. For instance, a field resembling a plane wave can be generated, to beam waves in a chosen direction. The established wave-field is then leaked out of the cavity through the semi-transparent interface (mask), which can also be spatially structured to further taper the emission of the leaky cavity. Due to the reflection from the semi-transparent interface of the cavity the wave undergoes multiply reflections inside the cavity and interacts with the metasurface more than one time. This increases the degree of freedom of the waveform generation inside the cavity. Also the weight of each single unit cell of the metasurface influencing field inside the cavity is increased.

Since the antenna simply relies on wave control, rather than wave emission, it is standard and protocol agnostic. The beamforming of the antenna does not result from the synchronization of many elementary sources, but rather on the shaping of a wavefield inside a cavity. That is, the same antenna can work for 5G mmWaves or Ka-band satellite communications without need to adapt the radiating elements or the feeding. The beamforming is realized in a passive way (the metasurface is DC active but RF passive). The antenna consumes very little of energy to beamform, like passive phased arrays. Yet it is much more efficient, since there are no dissipative circuits or materials to guide the waves, and can switch beams at the speed of electronics, like active phased arrays. Further, the cavity can be made of any shape, meaning that the antenna is perfectly conformable to any need. A simple 3D printing plus metal plating technology can be used for a cavity fabrication. Finally, this new antenna resembles a reflectarray or a transmitarray, yet it is much more compact, and presents numerous advantages over the later, that will be explained in the next part.

In the following, we concentrate on a prototype covering the satcom uplinks Ka frequency band (from 27.5 GHz to 31 GHz). The fabricated leaky cavity based antenna is depicted on Figure 2. The 4 cavity walls (6 mm thickness) are made using CNC-machining and screwed together to form a 106x106 mm^2 cavity. To improve the field homogenization in the cavity, its geometry is inspire from wave chaotic cavities.[13] The height of the cavity is $2.5\lambda = 25\ mm$ at 30 GHz. The metasurface is tightly attached to the bottom of the cavity and afterwards the antenna is closed with a semi-transparent mask formed as an array of conducting elements on a PCB substrate. The $10 \times 10cm^2$ metasurface represents a square array of 20x20 passive resonating patches placed each $\lambda/2$@30 GHz. The reflection phase of each resonator can be independently controlled for both polarisations with PIN diodes (see paper[14] for details on metasurface design and operation). The metasurface control is performed by means of FPGA control board. The control board is then connected to a PC with a LAN interface in order to perform the tuning of the metasurface properties and provide corresponding beamforming.

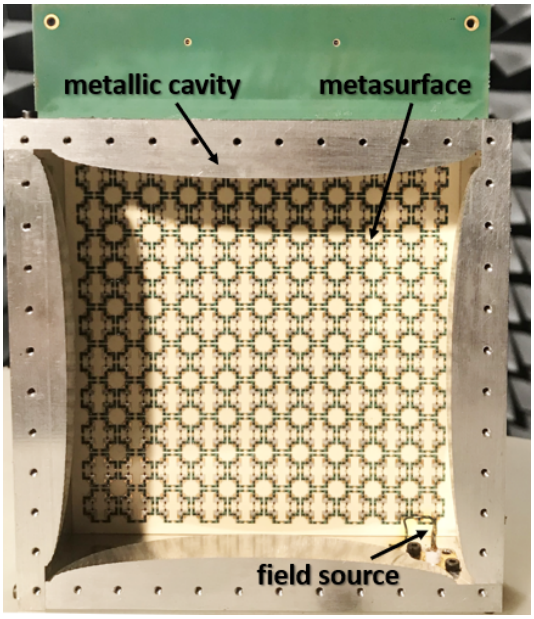

Figure 2: Photo of the an electronically reconfigurable leaky wave antenna with the semi-transparent mask removed.

One can see that the introduced design is quite robust and cheap for the fabrication. The most expensive part is the metasurface which is the set of passive resonators on a PCB substrate electrically controlled with PIN diodes. The metasurface is fabricated using the standard PCB technology and hence is ready for scaling for mass-production. For the given antenna size $10 \times 10\text{cm}^2$ metasurface has 800 PIN diodes (available from the market MACOM MADP-000907-14020x). Since each elements undergoes multiply reflections, the total number of diodes can be reduced without degrading a lot the parameters of the antenna. The antenna is able to adjust to the properties of the field source inside the cavity. This means that antenna can be fed by any type of source, waveguide or coaxial. That is the antenna is fully compatible with any RF equipment constituting any kind of frontend module and can be easily integrated with existing technology. The RF power accepted by the antenna is limited by the power handled by one PIN diode (+23 dBm) and can exceed 100 W for a $10 \times 10\text{cm}^2$ antenna comprising 800 PIN diodes. The antenna doesn't contain any moving parts and is highly resistant for vibration or temperature loads. The power consumption of the antenna is defined by the power consumption of the metasurface and control board. The highest power consumption occurs in the ON-state of the PIN diode and reaches only 4 W when all 800 PIN diodes are switched ON. Statistically during the antenna operation only half of the diodes are in ON state, so average power consumption is 2 W. In OFF state (antenna is idle) the consumption of metasurface is less than 0.35W. The power consumes by the 12 V control board is less than 1W. The control board itself can be powered from external USB power adaptor or use a separate power supply.

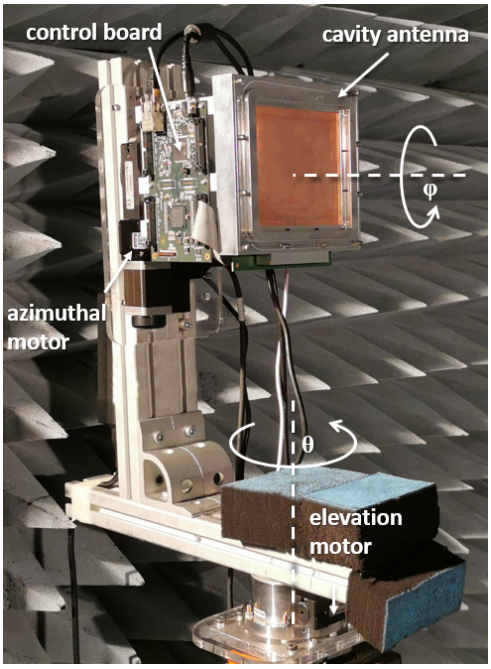

Figure 3: Experiment setup to measure antenna characteristics.

ANTENNA CHARACTERISTICS

The antenna is characterized in an anechoic chamber and a conical dual polarization horn antenna is used as a probe. The antenna is mounted on two rotational motors in the elevation over azimuth spherical setup[15] as shown in Figure 3. The distance between the antenna and the probe is 3 m, when the far-field region for a 10 cm × 10 cm at 30 GHz is at approximately 2 m. The radiation pattern is measured by means of a Vector Network Analyser (VNA). The antenna, the motors and the VNA were synchronized and controlled through a PC.

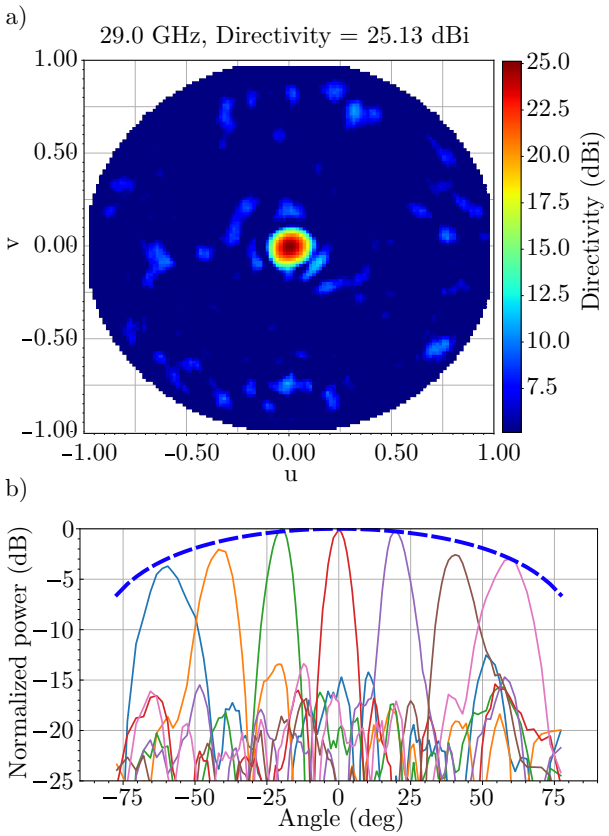

Figure 4: a) 3D radiation pattern of the antenna radiating at the boresight at 29 GHz. b) Measured scan loss of the antenna steering the beam from $-60°$ to $60°$.

Since the complexity of the antenna has been pushed from the hardware to the software domain, it is not possible to use common analytical beamforming. The predictive algorithm is being developed for the efficient and fast antenna beamforming. Currently the antenna is controlled by means of a close-loop optimization algorithm when a feedback from the VNA is used. A simple iterative procedure is developed following Vellekoop and Mosk.[16] In the first step all pixels are put in OFF-state. The state of the first pixel is flipped kept in ON-state, if the goal function increases. Otherwise, the pixel is flipped again back to OFF-state. This procedure is repeated with all pixels one by one and typically requires several loops over the metasurface. The optimization is terminated, when the goal function no longer increases during one loop of the optimization. Different goal functions can be used depending on desired functionality. For instance, the to create a single circularly-polarized beam, it is required to maximize $|S12_H \pm jS12_V|$, where $S12_{H,V}$ is the $S12$ parameter measured with the VNA for correspondingly horizontal and vertical polarization of the probe antenna. The plus or minus signs are chosen according to the desired circular polarization of the beam (left- or right-hand).

When the configuration of the metasurface is optimized for a desired functionality of the antenna, the return loss ($S11$) and the far-field radiation pattern are measured. By analyzing the radiation pattern a number of of antenna characteristics can be evaluated. Figure 4a) demonstrates the far-field radiation pattern (in terms of the directivity) of the antenna in the configuration optimized for boresight radiation. In direction cosine coordinates (u, v), the antenna directivity is calculated as follows:[17]

$$D(u,v) = \frac{4\pi P(u,v)}{\int \mathrm{d}u\mathrm{d}v P(u,v)/\sqrt{1-u^2-v^2}}, \tag{1}$$

where $P(u, v)$ is the measured power in the direction (u, v). The antenna directivity in this case constitutes approximately 25.1 dBi, when the theoretical maximum of the directivity for a 10 cm $\times$ 10 cm uniform aperture antenna is 30.7 dBi. The full width at half maximum (FWHM) of the beam is 6°. The maximum level of side-lobes is -17.5 dB, the average side-lobes level is -23.8 dB. The side-lobes level would be naturally better for a larger cavity and can be even more improved for the 10 cm$\times$10 cm by replacing for instance the simple localize monopole feed by a more complex source that better illuminate the metasurface and thus reduces the weight of uncontrolled radiation on the side-lobes.

The antenna efficiency measured is around 20% and is calculated by comparing directivity and gain measurements as defined by the International Standard.[18] The gain is measured by means of a reference horn antenna with a known value of the gain.[15] The efficiency of our prototype can be further increase by mitigating the dissipation of the metasurface. The new metasurfaces being developed at Greenerwave aimed for the dissipation level less than 1 dB.Metasurfacs base on such unit cells will allow to reduce the loss suffer by the EM wave at each bounce. Such 1 dB metasurface dissipation should lead to antenna efficiencies between 40% and 50%.

Futhermore, the developed antenna is an aperture antenna, which means that its radiation pattern is not a superposition of radiation of individual pixels constituting the metasurface. In comparison to classical phased-arrays, it allows one to significantly improve such parameters of the antenna as the scan loss. Indeed, Figure 4b) demonstrates the measured scan loss when the beam is steered from $-60°$ to $60°$. It is seen that the normalized power decreases by following all most perfectly the theoretical limit

of $\cos(\theta)^1$. It is here important to notice that the scan loss of our prototype follow a cosine law with no fitting coefficient. The angular step in this plot is 20°, but as small as 0.2° angular resolution was achieved.

Another advantage in comparison to phased-arrays is that the instantaneous bandwidth is software-controlled by simply updating the metasurface configuration. Figure 5a) demonstrates the ability of the antenna to change the instantaneous bandwidth from 100 MHz to 1 GHz. Importantly, within the whole 1 GHz bandwidth there is no beam-squint as Figure 5b) proves. In order to achieve the same characteristics with a phased-array, true time-delay RFICs are required, which are even more expensive and power consuming than common phase-shifters.

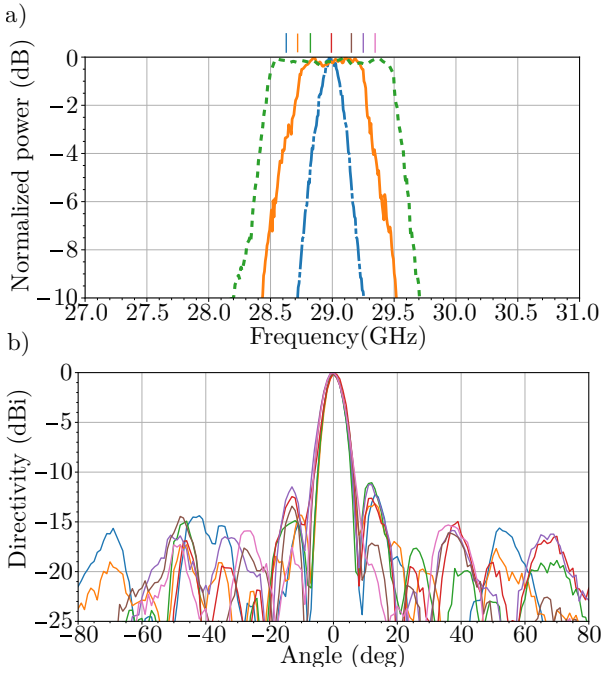

Figure 5: a) Frequency response of the antenna demonstrating software-controlled instantaneous bandwidth: from 100 MHz to 1 GHz. b) Radiation patterns at different frequencies (according to the colored bars on the panel a)) of the antenna radiating at the boresight and having the instantaneous bandwidth of 1 GHz. This panel demonstrates absence of the beam-squint effect.

Table 1: Antenna characteristics

Parameter	**Value**
Total bandwidth	> 4 GHz
Instantaneous bandwidth	100 MHz to 2 GHz
Efficiency	20 % (measured), 40 % (target)
Beamwidth	2°
Polarization	Software defined, horizontal, vertical, circular
Scan angle	+/- 70°
Scan loss	$\cos(\theta)^1$
Number of beams	Software controlled, any frequency, polarization, direction
Number of feeds	4 tested (hybrid beamforming)
Power consumption	2W average + 1W controller
Beam switching rate	> 100 kHz (depends on routing and control method)

To summarize the results presented in this section, let us underline a few aspects. First, the antenna is purely software controlled, both in terms of operational frequency, bandwidth, beam steering angle, the number of beams and their polarizations. The antenna is naturally limited by the bandwidth of the metasurface placed inside, which, however, can be very large (> 4 GHz for the current design at 30 GHz). The metasurface can also contain multiple pixels of optimized to operate at different frequency ranges, and that can be stacked. It means that the total operating bandwidth of a single aperture antenna can be made enormous. Next, for the beaming capabilities, it should be noted that the boundary conditions of the cavity are modified by the tunable metasurface to fulfil a given set of equations corresponding to a given wavefield. Therefore, the antenna can support any number of beams, very wide instantaneous bandwidths without any beam squint, has an ideal scan loss (that can be optimized with cavity shape, i.e. a conformal antenna can be desinged). In the following section, we demonstrate unique features of the developed antenna such as it can create 4 beams independently in 4 directions from 4 independent feeds, hence achieving naturally hybrid beamforming. All of this is of course limited by the number of degrees of freedom that the metasurface has. Table 1 summarizes measured principal characteristics of the 10 cm × 10 cm antenna prototype in the Ka-Tx frequency band.

In the previous section, we have assessed the reliability of our approach by the yardstick of the standard properties used to characterize any common electronically steerable antennas, regardless of the technology on which they are based. We have shown that our technology based on the combination of a leaky chaotic cavity and a reconfigurable metasurface has very good antenna properties that can be even more flexible and impressive than any other electronically steerable flat antenna (perfect scan loss, no beam squint, software controlled instantaneous bandwidth). But, our technology is much more agile and is not only limited to only improve standard antenna features. Indeed, some antenna's properties are inherent for the current technology only and are not (or barely not) achievable with common MMIC active antenna or passive array architectures. Indeed since the field emitted by the source is several time reflected toward the metasurface by the cavity wall, the antenna properties are not hampered by any array factor or particular field properties of the feeding. Unique behaviour of the generated beam are thus possible to achieve.

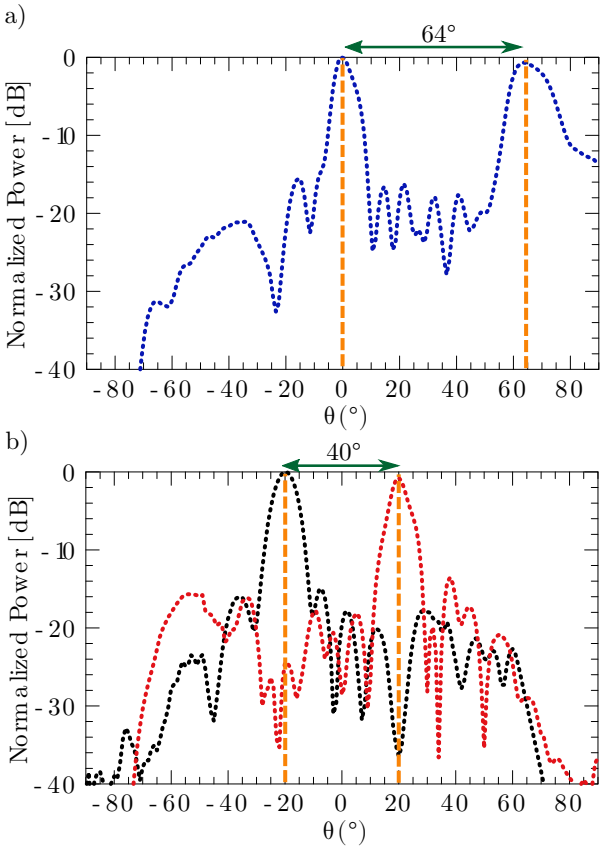

Figure 6: a) Radiation pattern of the antenna creating two beams at the same frequency and of the same polarization (RHCP). b) Radiation patterns of the antenna creating two beams at the same frequency and of the orthogonal polarizations (black curve – RHCP, and red curve – LHCP).

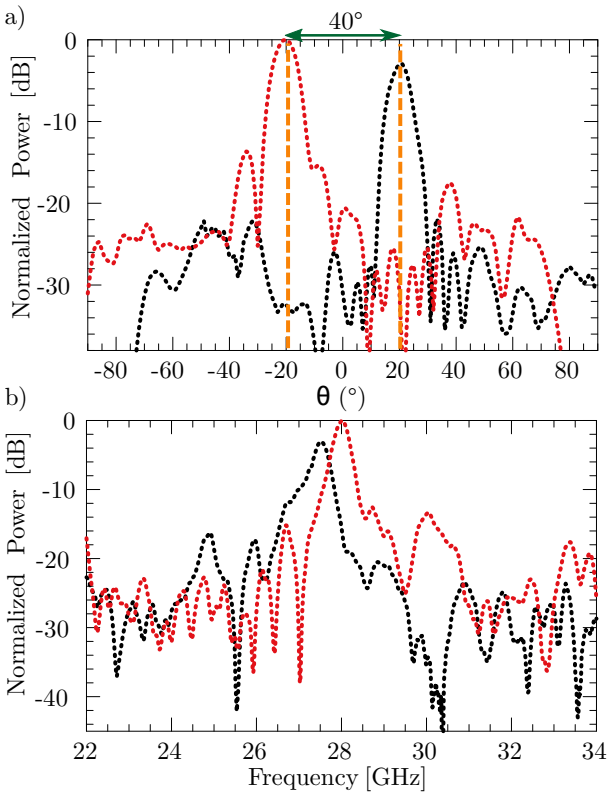

Figure 7: a) Radiation patterns of the antenna creating two beams at the different frequencies and orthogonal polarizations. b) Corresponding frequency response of the antenna for the orthogonal polarization. Black curves correspond to vertical polarization and red curves to horizontal polarization.

One of this unique properties is a true multi-beaming capabilities of the antenna. That means that with the same antenna it is possible to generate several beams with independent control of the polarisation / frequency / direction. To study this multi beaming capabilities, the experimental setup is modified in this way. We first place in the far field of our reconfigure antenna two dual polarized antennas spaced by an angle α. This receiving dual polarised antennas are connected two port 1 and 2 of a 4-port VNA and the port 3 is connected to the antenna under test. The measured polarization on the receiving horn antennas can be independently set to horizontal linear polarized (HP), vertical linear polarized (VP), left handed circular polarized (LHCP), or right handed circular polarized (RHCP). Then optimization process described in the previous section is performed in order to maximize the cost function, which reads as following:

$$\eta(c) = \max[|S_{13}^{p_1}(f_1, c)|^2 + |S_{23}^{p_2}(f_2, c)|^2], \quad (2)$$

where c is the metasurface configuration, p_1 and p_2 are the corresponding polarisations of the receiving horn antennas 1 and 2 and could be either HP, VP, LHCP or RHCP, and f_1 and f_2 are two optimization frequencies. When the optimization is done, we measure the radiation pattern corresponding to the best metasurface configuration. Results shown in Figure 6 demonstrate the measured 2D radiation pattern of the antenna generating two different beams at different directions and same frequency $f_1 = f_2 = 28\,\text{GHz}$. In Figure 6a, the two beam are 64° spaced and they are both RHCP ($p_1 = p_2$). We can observe that the properties of both beam almost don't degrade in comparison with single beam. The results shown on Figure 6b are obtained for $p_1 =$ RHCP and $p_2 =$ LCHP and $\alpha = 40°$. The black and red curves show respectively the radiation pattern measured on the RHCP and LHCP polarization. If we compare values both curves at the angles where they reach their maximum (vertical orange dashed curves), we notice that the cross-polarisation at corresponding frequencies is higher than 35 dB. We thus demonstrate the ability of our antenna to generate multi-beam having different propagation directions and orthogonal polarisations.

In Figure 7, we push the concept even further by generating with a single optimized configuration two beams having different propagation direction ($\alpha = 40°$), different polarisation ($p_1 \neq p_2$)and generated at two different frequencies ($f_1 = 27.5\,\text{GHz}$ $f_2 = 28\,\text{GHz}$) (see spectrum of Figure 7b). Note that f_1 and f_2 can be choose anywhere within the total bandwidth [27 GHZ, 31 Ghz]. In order to demonstrate the polarisation diversity of the antenna the beams generated in later configurations have linear orthogonal polarisations ($p_1 =$ VP and $p_2 =$ HP) contrary to the circular one for the beams presented on Figure 6. Figure 7a) shows in black doted curves the directive radiation pattern measured at 27.5 GHz on the VP polarisation and in red doted curves the directive radiation pattern measured at 28 GHz on the HP polarisation. The corresponding spectrum are shown in Figure 7b), where the black and red dotted curves are respectively the spectrum associated to VP and HP polarization. Even with this independent beamforming the properties of each beam are still good. But they are slightly degraded in comparison with single beam because of the finite number of degree of freedom provided by the metasurface and the increase of complexity of the cost function and the non optimised feeding of the cavity. We can notice that the presented feature can be used to provide simultaneous communication between satellite antenna, other satellites in constellation and ground

terminals and pave the way toward a full duplex single aperture antenna.

Multistreaming

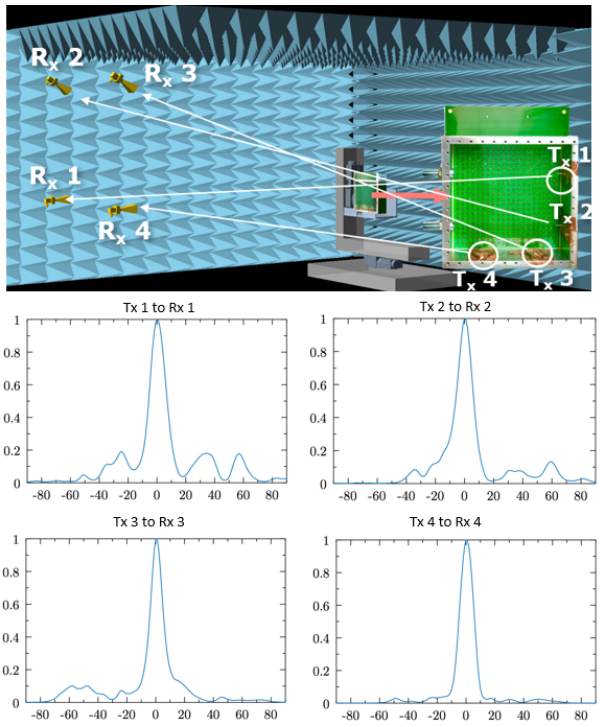

Figure 8: a) Setup of the MIMO experiment. b) Transmissions between different probe antennas and sources inside the cavity.

Another unique feature of the our concept is its ability to manage within a single cavity multistreaming from different transmitter inside the cavity toward different receiver outside. This complex feature is achieved at the sole cost of adding more ports (basically more monopole antennas) inside the cavity to feed it. No complex electronic neither complex sources are required. All the complexity is pushed to the software part, meaning the cost function used in the optimization process. To asses this properties we perform the experiment depicted in Figure 8a). We place inside a leaky reconfigurable cavity 4 monopole antenna label $\mathrm{Tx}_1, \mathrm{Tx}_2, \mathrm{Tx}_3$ and Tx_4 (as shown in the inset of Figure 8a)) and 4 receving horn antenna label $\mathrm{Rx}_1, \mathrm{Rx}_2, \mathrm{Rx}_3$ and Rx_4 in the far field inside an anechoic chamber. The four Tx_i antenna and the four Rx_i antenna are respectively connected to port 1 and 2 of a VNA trough SP4T switches. The leaky reconfigurable cavity antenna is placed as usual on scanning setup, that allow us to position it with respect to the Rx_i antennas. Then we optimize the metasurface configuration in a such a way that the power transmitted from antenna Tx_i to antenna Rx_i, $i \in [1,4]$ are maximized while power transmitted from antenna Tx_i to antenna Rx_j, $i \neq j$ are minimized. To do so, we use the following cost function

$$\eta_{c,\theta_o} = \max[\sum_{i=1}^{4} P^{\theta_o}_{\mathrm{Tx}_i \to \mathrm{Rx}_i}(c) - \sum_{i=1}^{4}\sum_{\substack{j=1 \\ j\neq i}}^{4} P^{\theta_o}_{\mathrm{Tx}_i \to \mathrm{Rx}_j}(c))] \tag{3}$$

where c is the metasurface configuration, θ_o the reference position of the cavity at which the optimisation is perform and $P^{\theta_o}_{\mathrm{Tx}_i \to \mathrm{Rx}_j}(c)$ stand for the power transmitted from monopole antenna Tx_i inside de cavity to horn antenna Rx_j outside. Finally, after optimization, we measured $P^{\theta}_{\mathrm{Tx}_i \to \mathrm{Rx}_i}(c)$ for $i \in [1,4]$ and $\theta \in [\theta_o - \pi/2, \theta_o + \pi/2]$. The result is shown in figure Figure 8b), where $P^{\theta}_{\mathrm{Tx}_1 \to \mathrm{Rx}_1}$, $P^{\theta}_{\mathrm{Tx}_2 \to \mathrm{Rx}_2}$, $P^{\theta}_{\mathrm{Tx}_3 \to \mathrm{Rx}_3}$ and $P^{\theta}_{\mathrm{Tx}_4 \to \mathrm{Rx}_4}$ are plotted as function of $\theta - \theta_o$. The 4 plot show 4 directive radiation patterns pointing toward 4 different receivers and corresponding to 4 independent streams handled by our antenna. This result illustrates the ability of our antenna to be used as a very simple system for real hybrid beamforming suitable for Multi-Satellite Multi-Users applications.[19]

Reduced number of pixel and beamforming capability robustness

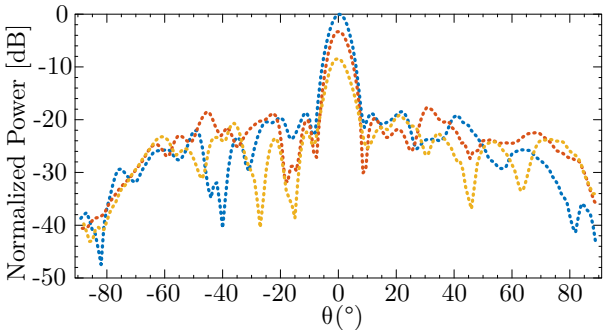

Figure 9: Beamforming capability robustness. Blue, Red, and oranges dotted curves are respectively optimization where 100%, 50% and 25% of the metasurface pixels are used. All the remaining pixel are let in OFF state. All curves are normalized with respect to the blue one

In this last section, we illustrate the robustness of the beamforming capability of our antenna with respect to the number of metasurface pixels available and their localization inside the cavity. To asses this unique feature, we perform the following experiment.

We first optimize the metasurface configuration in order the get a directive beam at boresight (blue dotted curves of Figure 9). Then, we randomly select half of the pixel. The non-selected pixel are put in OFF state and the selected ones are reused for optimization of the antenna at boresight. The optimized beam correspond with the red dotted curve of Figure 9. This experiment is repeated by selecting only a quarter of the pixel. The obtained radiation pattern is shown in orange dotted curve. In Figure 9, we can notice that the absolute level of side-lobes has not change. By reducing the number of pixel used, we have mainly reduced the gain in the direction of optimization by 3 dB when only 50% of pixel are used and by 9dB with 25% of pixel. This effect is well know from,[20] where it is shown that the maximum of power that can be controlled by a cavity is function of the number of degree of freedom available. The latter depend mainly on the number of pixel but also on the losses such as the metasurface dissipation. Therefore, lowering the metasurface losses, namely designing pixels with lower dissipation, is a way to mitigate the gain's decrease due to number of pixel reduction. Thus we have demonstrated that with our concept we are able to ensure beamforming properties even with a reduced number of pixel. The beamfroming capability is also not dependant of any particular position of the pixels inside the cavity. Futhermore, this result shows that we can use sparser metasurfaces that can be a way to even further reduce the final energy consumption and cost of the antenna. Another interesting consequence, is that our antenna can be self re-calibrating, meaning that, if at some point some diodes stop to work, the antenna will still be able to beamform.

Application: compensation of the dish reflector aberrations

The application of the unique concept of the leaky cavity antenna is not limited by shaping of the radiation from the source inside the cavity. In a similar manner the metasurface-controlled cavity can also modulate the radiation from the source positioned outside of the cavity and illuminating the cavity through the semi-transparent mask. In this configuration leaky cavity acts as a smart reflector which receives the signal from the external antenna and reflects it in the required direction modifing the properties of the reflected beam. But unlike common reflecting surface this smart reflector or *subreflector* posses much more degrees of freedom in controlling the reflected field. The cavity based subreflector can find applications in a space industry. Particularly it can be used for compensations of the aberrations of the beam reflected from the dish antenna. Reflectors for the parabolic dish antennas of the spacecrafts can have a folded construction to reduce space and weight during operation and launch. This reflectors suffer from a non-perfect reflecting surface which properties differ a lot from the properties of the common metallic parabolic reflector. The imperfections of the folded reflector cause aberrations of the reflected beam which can result in a strong degradation of the antenna properties. The compensation of this aberrations remains a challenge due to the complex probabilistic nature of the reflector distortion. The leaky cavity subreflector can be used in this case in order to compensate these aberrations and restore the properties of the antenna.

Schematically the operation of the subreflector is shown in Figure 10a). In a common parabolic reflector antenna the main beam is formed by the field emitted by a source (usually horn antenna) and reflected from the parabolic reflector (usually metallic parabolic dish). In case if reflector has a folded design, the imperfections of the dish surface give rise to a distortion of the reflected field and degradation of the antenna beam. To compensate the aberrations of the reflected fields, the electronically controlled subreflector is placed between the horn antenna and the distorted parabolic reflector. The beam from the source antenna first illuminates the subreflector (see Figure 10a), right). The waves penetrate inside the cavity through the semitransparent mask and interact with a metasurface inside. A multiple reflections inside the cavity occur in a similar manner as it was described in previous sections. An optimisation procedure is than implemented in order to select the cavity mode which will perform the best transformation of the incident field to compensate aberrations caused by non-perfect reflector surface and restore the beam of the main reflector.

Figure 10b) demonstrates 2D view of the analytically calculated radiation pattern of the common parabolic antenna with an ideal dish versus the radiation pattern in case if the surface of the dish contains some imperfections. The amplitude of the distortion of the dish surface in the analytical model reaches 5λ (at 30 GHz operating frequency). As one can see, the imperfections of the dish surface leads to strong degradation of the parameters of the antenna. In the bottom diagram of Figure 10b) the radiation pattern of a common dish reflector antenna is compared to the radiation pattern recovered by the subreflector. As one can see for the boresight beam the subreflector restores the power of the signal to the level more than 25dB in comparison with the distorted

one. Taking into account that subreflector is compact and can handle how power, it becomes a good candidate for space applications.

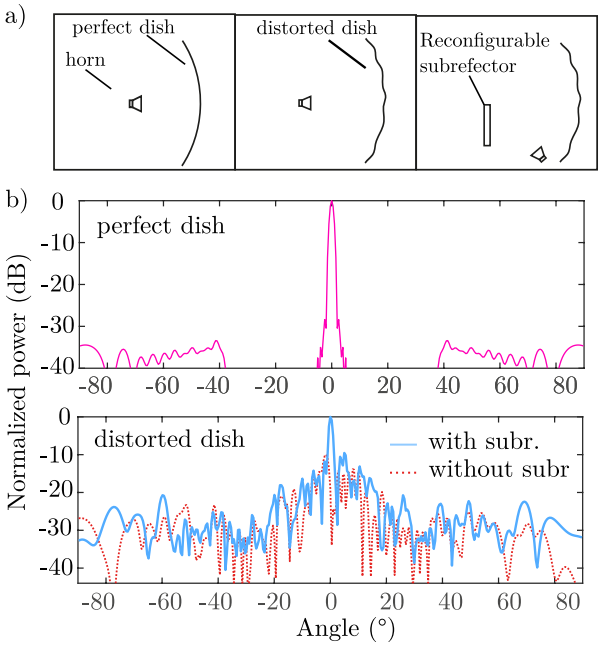

Figure 10: Schematics of the a) horn antenna with perfect dish, b) horn antenna with distorted dish, c) compensations of the dish aberrations. d) perfect versus distorted reflected signal from a dish, e) distorted versus compensated reflected signal from a dish antenna.

Conclusion

In this paper we have presented a very new concept of electronically reconfigurable leaky cavity antenna. The concept opens up the possibility to fabricating space compatible efficient, ultra low consumption electronically steerable antennas with extreme unique properties. The field inside the antenna is formed by a passive reflecting metasurface that provides ultra-low power consumption, below 3W average for a 10x10cm aperture antenna. The absence of dissipative RF-components makes it possible to increase the total antenna efficiency. The simple PCB technology and off-the-shelves components make the antenna cheap for fabrication, easy to spatialize and ready for mass production. Moreover the concept of the antenna allows a conformal shape fabrication that is highly convenient to use in for many applications, and made the concept very convenient for integration in complex systems such as satellite where each cm^3 are optimized.

We have shown experimentally that the compact and simple $10 \times 10 \times 2.5\,cm^3$ antenna can generate beams with any type of polarisation. Moreover it can provide a multibeaming functionality demonstrating fully independent software control of the direction, polarisation, and frequency band of each beam. The antenna is compatible with any frontend and can be easily upgrade for high power application.

It was also shown that the concept of the leaky cavity can be also implemented in a subreflector which transforms the reflected signal of the external antenna. We showed that this property can be used to compensate the aberrations of the folded parabolic dish antenna common for satellites.

We believe that the leaky wave cavity antenna technology developed by Greenerwave opens up a possibility for designing the very new type of antennas with unique properties. The presented here compact, fabrication-ready, robust antenna, which exhibits excellent scan loss, free of beam squint, performs multibeaming, independent software beam forming and beam control will be an excellent candidate for the space applications.

Acknowledgments

The authors acknowledge funding from the French AID "Agence Innovation Defense" under grant RAPID 3SFA, and funding from the French National Centre for Space Studies (CNES). We also thank Emmanuel Géron from ESPCI Paris for granting us permission to use measurement equipment.

References

[1] K. F. Braun. Electrical oscillations and wireless telegraphy. *Nobel Lecture*, Dec 1909.

[2] Guglielmo Marconi. Transmitting Electrical Signals, 1897.

[3] W. Roh, J.-Y. Seol, J. Park, B. Lee, J. Lee, Y. Kim, J. Cho, K. Cheun, and F. Aryanfar. Millimeter-wave beamforming as an enabling technology for 5g cellular communications: Theoretical feasibility and prototype results. *IEEE Communications Magazine*, 52(2):106–113, 2014. cited By 1693.

[4] W. Hong, Z.H. Jiang, C. Yu, J. Zhou, P. Chen, Z. Yu, H. Zhang, B. Yang, X. Pang, M. Jiang, Y. Cheng, M.K.T. Al-Nuaimi, Y. Zhang, J. Chen, and S. He. Multibeam antenna technologies for 5g wireless communications. *IEEE Transactions on Antennas and Propagation*, 65(12):6231–6249, 2017. cited By 308.

[5] C A Balanis. *Antenna Theory: Analysis and Design*. Wiley, 2016.

[6] K.F. Warnick, R. Maaskant, M.V. Ivashina, D.B. Davidson, and B.D. Jeffs. *Phased Arrays for Radio Astronomy, Remote Sensing, and Satellite Communications*. EuMA High Frequency Technologies Series. Cambridge University Press, 2018.

[7] R.J. Mailloux. *Phased Array Antenna Handbook, Third Edition*. Artech House antennas and electromagnetics analysis library. Artech House Publishers, 2017.

[8] N. Chahat. *CubeSat Antenna Design*. Wiley, 2021.

[9] Shuang Ma, Shao-Qing Zhang, Lei-Qiang Ma, Fan-Yi Meng, Daniel Erni, Lei Zhu, Jia-Hui Fu, and Qun Wu. Compact planar array antenna with electrically beam steering from backfire to endfire based on liquid crystal. *IET Microwaves, Antennas & Propagation*, 12(7):1140–1146, 2018.

[10] Denis J Connolly, Kul B Bhasin, and Robert R Romanofsky. (MMIC) Technology for Space Communications Applications. (Mmic), 1987.

[11] J. Huang, D. Rascoe, A.L. Riley, V. Lubecke, and L. Duffy. A ka-band mmic phased array antenna. In *Digest on Antennas and Propagation Society International Symposium*, pages 1212–1215 vol.3, 1989.

[12] Nadège Kaina, Matthieu Dupré, Geoffroy Lerosey, and Mathias Fink. Shaping complex microwave fields in reverberating media with binary tunable metasurfaces. *Scientific Reports*, 4(1):6693, Oct 2014.

[13] Jean-Baptiste Gros, Olivier Legrand, Fabrice Mortessagne, Elodie Richalot, and Kamardine Selemani. Universal behaviour of a wave chaos based electromagnetic reverberation chamber. *Wave Motion*, 51(4):664–672, jun 2014.

[14] Jean-Baptiste Gros, Vladislav Popov, Mikhail A. Odit, Vladimir Lenets, and Geoffroy Lerosey. A reconfigurable intelligent surface at mmwave based on a binary phase tunable metasurface. *IEEE Open Journal of the Communications Society*, pages 1–1, 2021.

[15] Jesper E Hansen. *Spherical near-field antenna measurements*, volume 26. IET, 1988.

[16] I.M. Vellekoop and A.P. Mosk. Phase control algorithms for focusing light through turbid media. *Optics Communications*, 281(11):3071–3080, 2008.

[17] Stuart Gregson, John McCormick, and Clive Parini. *Principles of planar near-field antenna measurements*, volume 53. IET, 2007.

[18] Antenna Standards Committee. *IEEE Standard Test Procedures for Antennas*, volume 23. 1981.

[19] Kai-Uwe Storek, Robert T. Schwarz, and Andreas Knopp. Multi-satellite multi-user mimo precoding: Testbed and field trial. In *ICC 2020 - 2020 IEEE International Conference on Communications (ICC)*, pages 1–7, 2020.

[20] Matthieu Dupré, Philipp del Hougne, Mathias Fink, Fabrice Lemoult, and Geoffroy Lerosey. Wave-Field Shaping in Cavities: Waves Trapped in a Box with Controllable Boundaries. *Phys. Rev. Lett.*, 115(1):017701, jul 2015.